

This discussion paper is/has been under review for the journal Hydrology and Earth System Sciences (HESS). Please refer to the corresponding final paper in HESS if available.

# Uncertainty contributions to low flow projections in Austria

J. Parajka<sup>1</sup>, A. P. Blaschke<sup>1</sup>, G. Blöschl<sup>1</sup>, K. Haslinger<sup>2</sup>, G. Hepp<sup>3</sup>, G. Laaha<sup>4</sup>, W. Schöner<sup>5</sup>, H. Trautvetter<sup>3</sup>, A. Viglione<sup>1</sup>, and M. Zessner<sup>3</sup>

<sup>1</sup>Institute for Hydraulic and Water Resources Engineering, TU Wien, Vienna, Austria

<sup>2</sup>Climate Research Department, Central Institute for Meteorology and Geodynamics, Vienna, Austria

<sup>3</sup>Institute for Water Quality, Resource and Waste Management, TU Wien, Vienna, Austria

<sup>4</sup>Institute of Applied Statistics and Computing, University of Natural Resources and Life Sciences (BOKU), Vienna, Austria

<sup>5</sup>Department of Geography and Regional Science, University of Graz, Graz, Austria

Received: 29 October 2015 – Accepted: 9 November 2015 – Published: 27 November 2015

Correspondence to: J. Parajka (parajka@hydro.tuwien.ac.at)

Published by Copernicus Publications on behalf of the European Geosciences Union.

HESSD

12, 12395–12431, 2015

Uncertainty  
contributions to low  
flow projections in  
Austria

J. Parajka et al.

Title Page

Abstract

Introduction

Conclusions

References

Tables

Figures

⏪

⏩

◀

▶

Back

Close

Full Screen / Esc

Printer-friendly Version

Interactive Discussion



## Abstract

The main objective of the paper is to understand the contributions to the uncertainty in low flow projections resulting from hydrological model uncertainty and climate projection uncertainty. Model uncertainty is quantified by different parameterizations of a conceptual semi-distributed hydrologic model (TUWmodel) using 11 objective functions in three different decades (1976–1986, 1987–1997, 1998–2008), which allows disentangling the effect of modeling uncertainty and temporal stability of model parameters. Climate projection uncertainty is quantified by four future climate scenarios (ECHAM5-A1B, A2, B1 and HADCM3-A1B) using a delta change approach. The approach is tested for 262 basins in Austria.

The results indicate that the seasonality of the low flow regime is an important factor affecting the performance of model calibration in the reference period and the uncertainty of  $Q_{95}$  low flow projections in the future period. In Austria, the calibration uncertainty in terms of  $Q_{95}$  is larger in basins with summer low flow regime than in basins with winter low flow regime. Using different calibration periods may result in a range of up to 60 % in simulated  $Q_{95}$  low flows.

The low flow projections show an increase of low flows in the Alps, typically in the range of 10–30 % and a decrease in the south-eastern part of Austria mostly in the range –5 to –20 % for the period 2021–2050 relative the reference period 1976–2008. The change in seasonality varies between scenarios, but there is a tendency for earlier low flows in the Northern Alps and later low flows in Eastern Austria. In 85 % of the basins, the uncertainty in  $Q_{95}$  from model calibration is larger than the uncertainty from different climate scenarios. The total uncertainty of  $Q_{95}$  projections is the largest in basins with winter low flow regime and, in some basins, exceeds 60 %. In basins with summer low flows and the total uncertainty is mostly less than 20 %. While the calibration uncertainty dominates over climate projection uncertainty in terms of low flow magnitudes, the opposite is the case for low flow seasonality. The implications of the uncertainties identified in this paper for water resources management are discussed.

## Uncertainty contributions to low flow projections in Austria

J. Parajka et al.

Title Page

Abstract

Introduction

Conclusions

References

Tables

Figures



Back

Close

Full Screen / Esc

Printer-friendly Version

Interactive Discussion



# 1 Introduction

Understanding climate impacts on hydrologic water balance in general and extreme flows in particular is one of the main scientific interests in hydrology. Stream flow estimation during low flow conditions is important also for a wide range of practical applications, including estimation of environmental flows, effluent water quality, hydropower operations, water supply or navigation. Projections of low flows in future climate conditions are thus essential for planning and development of adaptation strategies in water resources management. However it is rarely clear how the uncertainties in assumptions used in the projections translate into uncertainty of estimated future low flows.

There are numerous regional and national studies that have analyzed the effects of climate change on the stream flow regime, including low flows (e.g. Feyen and Dankers, 2009; Prudhomme and Davies, 2009; Chauveau et al., 2013, among others). Most of them apply outputs from different global or regional climate circulation models, which are based on different emission scenarios. The projections of low flows are then typically simulated by hydrologic models of various complexity. Only few studies, however, evaluate the uncertainty of low flow projections and the relative contribution of its different sources (i.e. climate projection, hydrologic model structure and/or model parameterizations). Such studies include assessment of the impact of different climate projections on low flows evaluated e.g. in Huang et al. (2013) and Forzieri et al. (2014). While Huang et al. (2013) assesses the low flow changes and uncertainty in the five largest river basins in Germany, Forzieri et al. (2014) evaluates the uncertainty of an ensemble of 12 bias corrected climate projections in the whole of Europe. Both studies quantify uncertainty in terms of the number of low flow projections that suggest the same change direction. Their results indicate a consistent pattern of low flow changes across different regions in Europe. A common feature of such ensemble climate scenarios is an increase in the agreement between ensemble members with increasing future time horizon of climate projections. The impact of hydrologic model structure and climate projections was evaluated in Dams et al. (2015). They applied four hydrologic

## HESSD

12, 12395–12431, 2015

### Uncertainty contributions to low flow projections in Austria

J. Parajka et al.

Title Page

Abstract

Introduction

Conclusions

References

Tables

Figures



Back

Close

Full Screen / Esc

Printer-friendly Version

Interactive Discussion





hydrologic model calibration, the model is first calibrated by using observed climate characteristics in the reference period. In a next step, RCM outputs are used to estimate monthly differences between simulations in the reference (control) and future periods. These differences (delta changes) are then added to the observed model inputs and used for simulating future hydrologic changes. The difference between simulations of a hydrologic model in the reference and future periods are then used to interpret potential impacts of changing climate on future river flows.

Here we apply the delta change approach to simulate daily flows in the future period. The future low flow changes are quantified by the  $Q_{95}$  low flow quantile and seasonality index SI. The  $Q_{95}$  represents river flow that is exceeded on 95% of the days of the entire reference or future period. This characteristic is one of the low flow reference characteristic which is widely used in Europe (Laaha and Blöschl, 2006). Seasonality index SI represents the average timing of low flows within a year (Laaha and Blöschl, 2006, 2007). It is estimated from the Julian dates  $D_j$  of all days when river flows are equal or below  $Q_{95}$  in the reference or future periods.  $D_j$  represents a cyclic variable. Its directional angle, in radians, is given by:

$$\theta_j = \frac{D_j \times 2\pi}{365}. \quad (1)$$

The arithmetic mean of Cartesian coordinates  $x_\theta$  and  $y_\theta$  of a total of  $n$  single days  $j$  is defined as:

$$\begin{aligned} x_\theta &= \frac{1}{n} \sum_j \cos(\theta_j) \\ y_\theta &= \frac{1}{n} \sum_j \sin(\theta_j). \end{aligned} \quad (2)$$

**Uncertainty contributions to low flow projections in Austria**

J. Parajka et al.

Title Page

Abstract

Introduction

Conclusions

References

Tables

Figures

⏪

⏩

◀

▶

Back

Close

Full Screen / Esc

Printer-friendly Version

Interactive Discussion



From this, the directional angle of the mean vector may be calculated by:

$$\theta = \arctan\left(\frac{y_\theta}{x_\theta}\right) \quad \text{1st and 4th quadrant: } x > 0 \quad (3)$$
$$\theta = \arctan\left(\frac{y_\theta}{x_\theta}\right) + \pi \quad \text{2nd and 3rd quadrant: } x < 0.$$

Finally, the mean day of occurrence is obtained from re-transformation to Julian Date:

$$SI = \theta \times \frac{365}{2\pi}, \quad (4)$$

5 and the variability of the date of occurrence about the mean date (i.e. seasonality strength) is characterized by the length parameter  $r$ . The parameter  $r$  is estimated as (Burn, 1997):

$$r = \sqrt{\overline{x^2} + \overline{y^2}} / n, \quad (5)$$

10 and ranges from  $r = 0$  (low strength, uniform distribution around the year) to  $r = 1$  (maximum strength, all extreme events of floods occur on the same day).

The SI index is estimated for observed flows and flows simulated by a hydrologic model. The difference between model simulations (i.e.  $Q_{95}$  and SI estimates) in the reference and future periods are then used to quantify potential impacts of climate change on low flows. Both  $Q_{95}$  and SI measures are estimated by the lfstat package in R software (Koffler and Laaha, 2014).

15

## 2.2 Hydrologic model

Low flow projections are estimated by a conceptual semi-distributed rainfall runoff model (TUWmodel, Viglione and Parajka, 2014). The model simulates water balance components on a daily time step by using precipitation, air temperature and potential

evaporation data as an input. The model consists of three modules which allow simulating changes in snow, soil storages and groundwater storages. More details about the model structure and examples of application in the past are given e.g. in Parajka et al. (2007, 2008), Viglione et al. (2013) and Ceola et al. (2015).

In this study, the TUWmodel is calibrated by using the SCE-UA automatic calibration procedure (Duan et al., 1992). The objective function ( $Z_Q$ ) used in calibration is selected on the basis of prior analyses performed in different calibration studies in the study region (see e.g. Parajka and Blöschl, 2008; Merz et al., 2011). It consists of weighted average of two variants of Nash–Sutcliffe model efficiency,  $M_E$  and  $M_E^{\log}$ .

While the  $M_E$  efficiency emphasize the high flows, the  $M_E^{\log}$  efficiency accentuates more the low flows. The maximized objective function  $Z_Q$  is defined then as

$$Z_Q = w_Q \times M_E + (1 - w_Q) \times M_E^{\log}, \quad (6)$$

where  $w_Q$  represents the weight on high or low flows. If  $w_Q$  equals 1 then the model is calibrated to high flows, if it equals to 0 then to low flows only.  $M_E$  and  $M_E^{\log}$  are estimated as

$$M_E = 1 - \frac{\sum_{i=1}^n (Q_{\text{obs},i} - Q_{\text{sim},i})^2}{\sum_{i=1}^n (Q_{\text{obs},i} - \overline{Q_{\text{obs}}})^2} \quad (7)$$

$$M_E^{\log} = 1 - \frac{\sum_{i=1}^n (\log(Q_{\text{obs},i}) - \log(Q_{\text{sim},i}))^2}{\sum_{i=1}^n (\log(Q_{\text{obs},i}) - \overline{\log(Q_{\text{obs}})})^2} \quad (8)$$

where  $Q_{\text{sim},i}$  is the simulated discharge on day  $i$ ,  $Q_{\text{obs},i}$  is the observed discharge,  $\overline{Q_{\text{obs}}}$  is the average of the observed discharge over the calibration (or verification) period of  $n$  days.

## HESSD

12, 12395–12431, 2015

### Uncertainty contributions to low flow projections in Austria

J. Parajka et al.

Title Page

Abstract

Introduction

Conclusions

References

Tables

Figures

⏪

⏩

◀

▶

Back

Close

Full Screen / Esc

Printer-friendly Version

Interactive Discussion



## 2.3 Uncertainty estimation

The uncertainty defined as the range of low flow projections is evaluated for two contributions. The first analyses the uncertainty (i.e. the range of  $Q_{95}$  and SI) estimated for different variants of hydrologic model calibration. Here, two cases are evaluated. In order to assess the impact of time stability of model parameters (Merz et al., 2011), TUWmodel is calibrated separately for three different decades (1976–1986, 1987–1997, 1998–2008). The effect of objective function used for the TUWmodel calibration is evaluated by comparing 11 variants of weights ( $w_Q$ ) used in  $Z_Q$ . Following  $w_Q$  are tested: 0.0, 0.1, 0.2, 0.3, 0.4, 0.5, 0.6, 0.7, 0.8, 0.9 and 1.0. The hydrologic model is calibrated for all 11 variants in each selected decade. Calibrated models are then used for flow simulations and hence  $Q_{95}$  and SI estimation in the entire reference period 1976–2008.

The second contribution evaluates the uncertainty of  $Q_{95}$  and SI changes simulated for different climate scenarios. The effect of calibration uncertainty (case 1) is compared for four selected climate scenarios (more details are given in Data section). The delta change approach is used for simulation of future river flows in the period 2021–2050 relative to the reference period 1987–2008. The delta changes of  $Q_{95}$  and SI values between reference and future periods are estimated for four selected climate scenarios, 11 variants of model calibration and three selected decades. The relative contribution of the impact of model calibration (i.e. time stability and objective function selection) and climate scenario is then evaluated seasonally at the regional scale.

## 3 Data

Study region is Austria (Fig. 1). Austria represents diverse climate and physiographic conditions of Central Europe, which is reflected in different hydrologic regimes (Gaál et al., 2012). The topography varies from 115 m.a.s.l. in the lowlands to more than 3700 m.a.s.l. in the Alps. Austria is located in a temperate climate zone influenced

HESSD

12, 12395–12431, 2015

### Uncertainty contributions to low flow projections in Austria

J. Parajka et al.

Title Page

Abstract

Introduction

Conclusions

References

Tables

Figures

⏪

⏩

◀

▶

Back

Close

Full Screen / Esc

Printer-friendly Version

Interactive Discussion



by the Atlantic, meridional south circulation and the continental weather systems of Europe. Mean annual air temperature varies between  $-8$  to  $10^{\circ}\text{C}$ . The mean annual precipitation ranges from  $550\text{ mm year}^{-1}$  in the Danube lowlands, to more than  $3000\text{ mm year}^{-1}$  on the windward slopes of the Alps.

The analysis is based on daily river flow measurements at 262 gauges (Fig. 1). This dataset represents a subset of data used in Laaha and Blöschl (2006), which consists of gauges for which hydrographs are not seriously affected by abstractions and karst effects during the low flow periods. Figure 1 shows two main low flow regimes in Austria. While orange and red colours indicate 130 stations with dominant summer low flow occurrence, blue colour indicates 132 gauges with winter flow minima. These two groups represent basins with distinct low flow seasons, which are controlled by different hydrologic processes. While the winter flow minima in the mountains are controlled by freezing processes and snow storage, summer low flows occur during long-term persistent dry periods when evaporation exceeds precipitation. The different low flow generating processes, together with the hydro-climatic variety of the study area, gives rise to an enormous spatial complexity of low flows in Austria. The largest values occur in the high precipitation areas in the Alps, with typical values ranging from  $6$  to  $20\text{ L s}^{-1}\text{ km}^{-2}$ . The lowest values occur in the east ranging from  $0$  to  $8\text{ L s}^{-1}\text{ km}^{-2}$ , although the spatial pattern is much more intricate.

Climate data used in hydrologic modeling consists of mean daily precipitation and air temperature measurements at 1091 and 212 climate stations in the period 1976–2008, respectively. Model inputs have been prepared by spatial interpolation and zonal averaging described in detail in previous modeling studies (please see e.g. Merz et al., 2011 or Parajka et al., 2007). These data serve as a basis for hydrologic model calibration and as a reference for future delta change simulations. Figure 2 shows basin averages of mean annual air temperature, precipitation and runoff in the period 1976–2008. The thin lines represent the medians of climate characteristic over the averages of basins with summer and winter low flows. The thick lines represent the average over the three selected decades. The two groups of basins differ clearly in the climate

## HESSD

12, 12395–12431, 2015

### Uncertainty contributions to low flow projections in Austria

J. Parajka et al.

Title Page

Abstract

Introduction

Conclusions

References

Tables

Figures



Back

Close

Full Screen / Esc

Printer-friendly Version

Interactive Discussion



# HESSD

12, 12395–12431, 2015

## Uncertainty contributions to low flow projections in Austria

J. Parajka et al.

[Title Page](#)[Abstract](#)[Introduction](#)[Conclusions](#)[References](#)[Tables](#)[Figures](#)[⏪](#)[⏩](#)[◀](#)[▶](#)[Back](#)[Close](#)[Full Screen / Esc](#)[Printer-friendly Version](#)[Interactive Discussion](#)

regime. Basins with summer low flows are characterized by higher air temperatures, less precipitation and less runoff. The comparison of three different decades indicates that mean annual air temperatures have increased by 1 °C in the period 1976–2008. This increase is similar for both groups of basins. Interestingly, the mean annual precipitation has increased over the last three decades, which is likely compensated by increased evapotranspiration, as the mean annual runoff remains rather constant.

The regional climate model (RCM) scenarios used in this study are based on the results of the reclip.century project (Loibl et al., 2011). The ensemble climate projections are represented by COSMO-CLM RCM runs forced by the ECHAM5 and HADCM3 global circulation models for three different IPCC emission scenarios (A1B, B1 and A2, Nakicenovic et al., 2000). These represent a large spread of different emission pathways from a “business as usual” scenario with prolonged greenhouse gas emissions (A2), a scenario with moderate decline of emissions after 2050 (A1B) and a scenario indicating considerably reduced emissions from now on (B1). The decision on the two driving GCMs is justified by an analysis of Prein et al. (2008) who investigated the skill of the CMIP3 GCM ensemble over Central Europe and show that these two models are among the best performing ones.

Table 1 summarizes the annual and seasonal differences (delta changes) of mean basin precipitation and air temperature between the future (2021–2050) and reference (1976–2006) periods. Table 1 indicates that the largest warming is obtained by simulations driven by HADCM3. The median of air temperature increase in summer exceeds 2 °C. In numerous basins, a small decrease in air temperature in winter is simulated by ECHAM5 A2 and B1 simulations. The changes in mean annual precipitation are within the range  $\pm 9\%$  in all selected basins. The increase tends to be larger in winter than in the summer period.





low flow period, when the model parameterization does not allow to fit well some small rainfall–runoff events in the summer or autumn, which interrupt the observed low flow period but not the flows simulated by the hydrologic model (i.e. the precipitation event is completely absorbed by the soil storage of the model and does not contribute to the runoff generation).

The spatial pattern of the uncertainty of  $Q_{95}$  estimation in the reference period 1976–2008 is presented in Fig. 6. Figure 6 shows the range of differences between simulated and observed  $Q_{95}$  for the different calibration variants. Left panels show the range for model calibrations performed by the same objective function (i.e. top left panel –  $w_Q = 0.5$  and bottom left panel –  $w_Q = 0.0$ ) used for calibration in the three different calibration periods (1976–1986, 1987–1997, 1998–2008). Contrary, right panels show the range of differences for one calibration period but between 11 variants of the objective function ( $w_Q$ ) (i.e. top right panel – 1976–1986, bottom right panel – 1998–2008). The results indicate that the  $Q_{95}$  differences vary more between the different objective functions (right panels), however in many basins the range exceeds 60% even if the model is calibrated by one objective function but in the different calibration periods. As already indicated in Fig. 4, the differences are larger in basins with the summer low flows, particularly for variants calibrated in the period 1976–1986. For particular basin, the differences are not strongly related to the weight  $w_Q$  used in the calibration, with an exception of  $w_Q = 1$ , which tends to have the largest difference to observed  $Q_{95}$ . Some examples of the model performance for individual basins are given in companion paper of Laaha et al. (this issue).

Spatial variability of the model uncertainty in terms of low flow seasonality is presented in Fig. 7. Figure 7 shows, similarly as Fig. 6, the range of differences between the simulated and observed SI for different calibration variants. The results clearly indicate that basins with the winter low flow regime (i.e. situated in the Alps) vary significantly less for different calibration settings than the basins with the summer low flow regime. The range of differences is typically less than 14 days in the mountains, compared to more than 90 days in many basins with the summer regime.

## Uncertainty contributions to low flow projections in Austria

J. Parajka et al.

[Title Page](#)[Abstract](#)[Introduction](#)[Conclusions](#)[References](#)[Tables](#)[Figures](#)[⏪](#)[⏩](#)[◀](#)[▶](#)[Back](#)[Close](#)[Full Screen / Esc](#)[Printer-friendly Version](#)[Interactive Discussion](#)



nificantly smaller than obtained for different calibration variants in the reference period (Fig. 4).

Examples of spatial patterns of low flow projections are presented in Fig. 9 and 10. The projections of  $Q_{95}$  changes (Fig. 9) indicate an increase of low flows in the Alps, typically in the range of 10–30 %. A decrease is simulated in south-eastern part of Austria (Styria) mostly in the range of –5 to –20 %. The most spatially different projection is provided by the AIT HADCM3 A1B climate scenario which simulates the strongest gradient between an  $Q_{95}$  increase in the Alps in winter and a decrease in south-eastern part in summer. The change in the seasonality varies between the scenarios, but there is a tendency for earlier low flows in the Northern Alps and a shift to later occurrence of low flows in the Eastern Austria. As already indicated in Fig. 8, the shift in seasonality is larger than one month only in a few basins.

Figures 9 and 10 show projections of low flows for four climate scenarios, but only one variant of hydrologic model parameters. The evaluation of the impacts of different calibration variants on the variability of low flow projections is presented in Figs. 11 and 12. These Figures indicate the range of  $Q_{95}$  (Fig. 11) and the seasonality occurrence (Fig. 12) changes obtained by 11 calibration variants and three calibration periods. The range of  $Q_{95}$  changes is interestingly the largest in basins with the winter low flow regime. In the Alps, the increase of  $Q_{95}$  is often in the range of 15 % to more than 60 %. On the other hand, the future  $Q_{95}$  estimates vary only slightly between the calibration variants in basins with the summer low flows. In most of the basins is the change less than 20 %. The impact of the selection of objective function is, however, much larger for the estimation of the seasonality changes. Depending on the calibration variant, the change in seasonality can vary within more than 3 months, e.g. in the south-eastern part of Austria.

The total uncertainty of low flow projections of  $Q_{95}$  and SI is presented in Fig. 13. While the top panels show the range of low flow characteristics for all climate scenarios, calibration variants and periods, the bottom panels show the ratio between the uncertainty of future low flow projections to the calibration uncertainty in the reference

## Uncertainty contributions to low flow projections in Austria

J. Parajka et al.

Title Page

Abstract

Introduction

Conclusions

References

Tables

Figures



Back

Close

Full Screen / Esc

Printer-friendly Version

Interactive Discussion















## Uncertainty contributions to low flow projections in Austria

J. Parajka et al.

Title Page

Abstract

Introduction

Conclusions

References

Tables

Figures

⏪

⏩

◀

▶

Back

Close

Full Screen / Esc

Printer-friendly Version

Interactive Discussion



Prudhomme, C., and Davies, H.: Assessing uncertainties in climate change impact analyses on the river flow regimes in the UK, Part 2: future climate, *Climatic Change*, 93, 177–195, doi:10.1007/s10584-008-9464-3, 2009.

5 Skoien, J. O., Blöschl, G., Laaha, G., Pebesma, E., Parajka, J., and Viglione, A.: rtop: an R package for interpolation of data with a variable spatial support, with an example from river networks, *Comput. Geosci.*, 67, 180–190, doi:10.1016/j.cageo.2014.02.009, 2014.

Van der Linden, P. and Mitchell, J. F. B. (Eds.): *ENSEMBLES: Climate Change and its Impacts: Summary of Research and Results from the ENSEMBLES Project*, Met Office Hadley Centre, Exeter, UK, 160 pp., 2009.

10 Van Loon, A. F. and Van Lanen, H. A. J.: A process-based typology of hydrological drought, *Hydrol. Earth Syst. Sci.*, 16, 1915–1946, doi:10.5194/hess-16-1915-2012, 2012.

Van Loon, A. F., Ploum, S. W., Parajka, J., Fleig, A. K., Garnier, E., Laaha, G., and Van Lanen, H. A. J.: Hydrological drought types in cold climates: quantitative analysis of causing factors and qualitative survey of impacts, *Hydrol. Earth Syst. Sci.*, 19, 1993–2016, doi:10.5194/hess-19-1993-2015, 2015.

15 Viglione, A. and Parajka, J.: T UWmodel: Lumped Hydrological Model for Education Purposes, R package version 0.1-4, available at: <http://CRAN.R-project.org/package=TUWmodel>, (last access: 20 November 2015), 2014.

Viglione, A., Parajka, J., Rogger, M., Salinas, J. L., Laaha, G., Sivapalan, M., and Blöschl, G.: Comparative assessment of predictions in ungauged basins – Part 3: Runoff signatures in Austria, *Hydrol. Earth Syst. Sci.*, 17, 2263–2279, doi:10.5194/hess-17-2263-2013, 2013.

20 Zessner, M.: Transboundary pollution and water quality policies in Austria, *Water Sci. Technol.*, 58, 1917–1923, doi:10.2166/wst.2008.562, 2008.



# HESSD

12, 12395–12431, 2015

## Uncertainty contributions to low flow projections in Austria

J. Parajka et al.

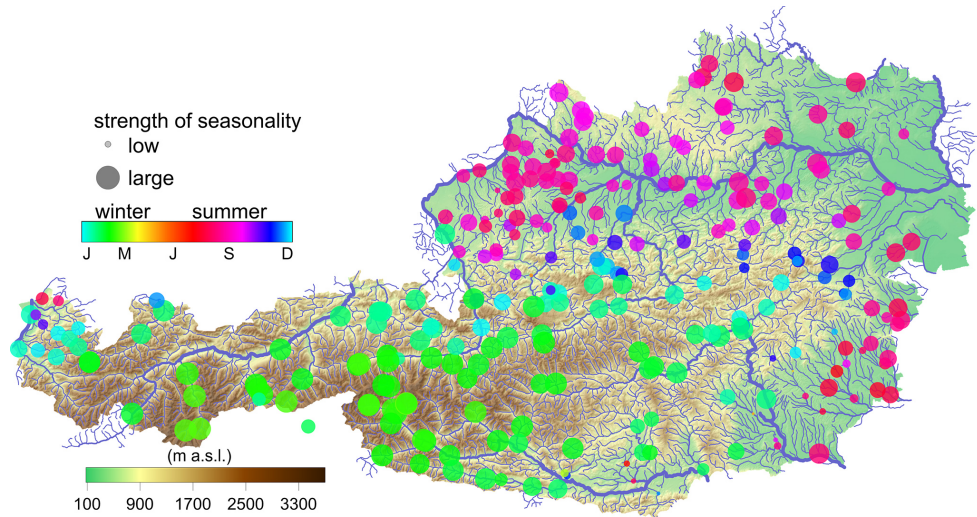


**Figure 1.** Topography of Austria and location of 262 river flow gauges. Colour and symbol size of the gauges represents seasonality of low flows SI and its strength ( $r$ ) in the period 1976–2008, respectively. The SI and its strength is estimated by R lfstat package (Koffler and Laaha, 2014).

[Title Page](#)[Abstract](#)[Introduction](#)[Conclusions](#)[References](#)[Tables](#)[Figures](#)[◀](#)[▶](#)[◀](#)[▶](#)[Back](#)[Close](#)[Full Screen / Esc](#)[Printer-friendly Version](#)[Interactive Discussion](#)

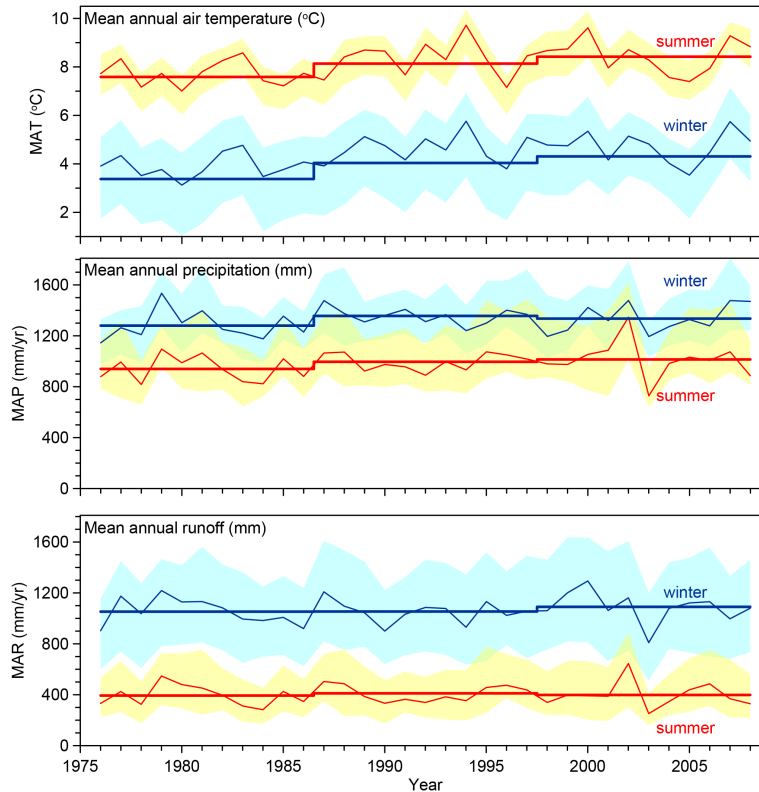


**Figure 2.** Mean annual air temperature (MAT, top), precipitation (MAP, middle) and runoff (MAR, bottom) for basins with summer (yellow/red) and winter (blue) low flow minima (Fig. 1). Thin lines represent the median of mean annual values of MAT, MAP and MAR. Thick lines indicate the average for each of the three periods: 1976–86, 1987–97 and 1998–2008. Scatter (i.e. 75 and 25% percentiles) indicates the variability between the basins.

**Uncertainty contributions to low flow projections in Austria**

J. Parajka et al.

[Title Page](#)

[Abstract](#) | [Introduction](#)

[Conclusions](#) | [References](#)

[Tables](#) | [Figures](#)

[◀](#) | [▶](#)

[◀](#) | [▶](#)

[Back](#) | [Close](#)

[Full Screen / Esc](#)

[Printer-friendly Version](#)

[Interactive Discussion](#)



## Uncertainty contributions to low flow projections in Austria

J. Parajka et al.

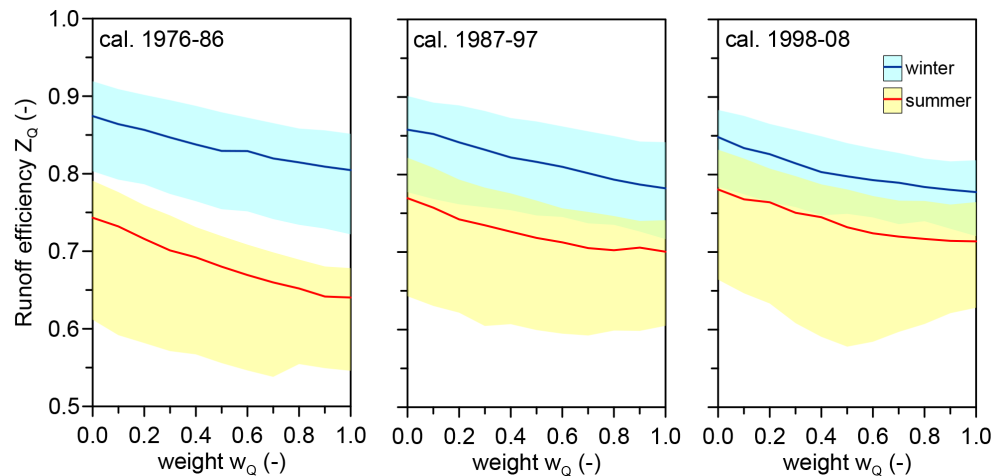


**Figure 3.** Runoff model efficiency ( $Z_Q$ ) for different calibration weights  $w_Q$  in three different calibration periods. Lines represent the medians, scatter (i.e. 75–25% percentiles) shows the  $Z_Q$  variability over basins with dominant winter (blue) and summer (orange) low flow regime.

[Title Page](#)[Abstract](#)[Introduction](#)[Conclusions](#)[References](#)[Tables](#)[Figures](#)[⏪](#)[⏩](#)[◀](#)[▶](#)[Back](#)[Close](#)[Full Screen / Esc](#)[Printer-friendly Version](#)[Interactive Discussion](#)

## Uncertainty contributions to low flow projections in Austria

J. Parajka et al.

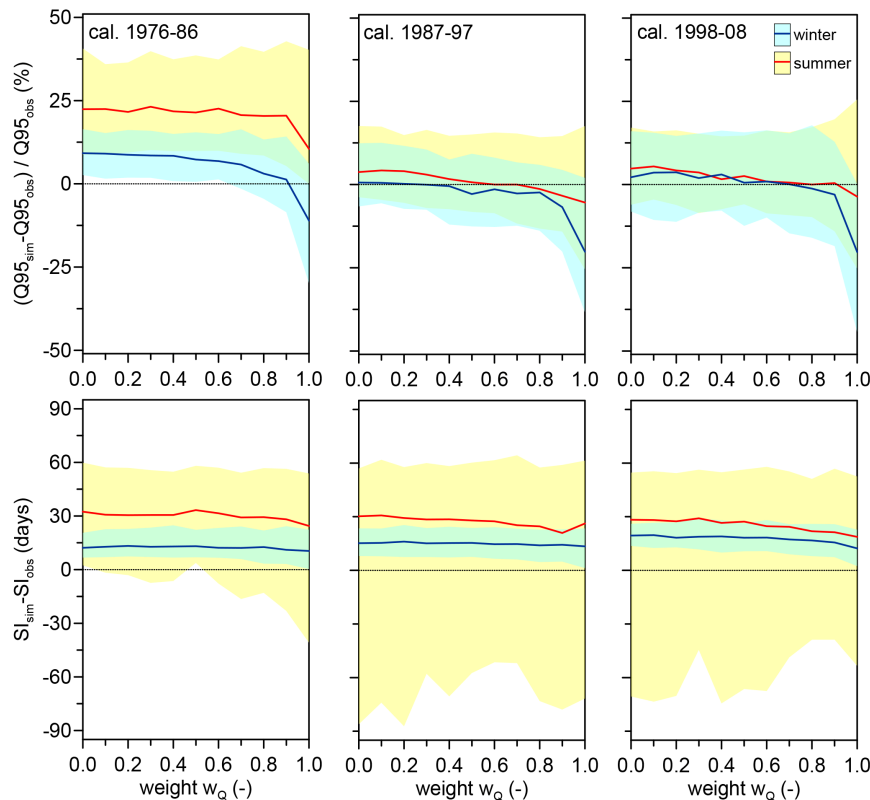


**Figure 4.** Difference between simulated and observed low flow characteristics (top panels low flow quantile  $Q_{95}$ , bottom panels seasonality index  $SI$ ) for different calibration variants ( $w_Q$ ) and calibration periods. Lines represent the median, scatter (i.e. 75–25% percentiles) show the variability over basins with dominant winter (blue) and summer (orange) low flow regime. The differences are estimated between model simulations and observations in the entire reference period 1976–2008.

## Uncertainty contributions to low flow projections in Austria

J. Parajka et al.

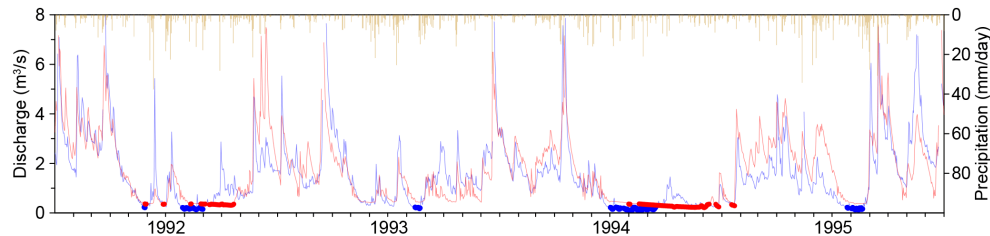


**Figure 5.** Comparison of observed (blue) and simulated (red) flow for Hoheneich/Braunaubach, 291.5 km<sup>2</sup>). Thick lines show flows below low flow quantile  $Q_{95}$ . Model simulations are based on calibration variant  $w_Q = 0.5$  in the period 1998–2008.

[Title Page](#)[Abstract](#)[Introduction](#)[Conclusions](#)[References](#)[Tables](#)[Figures](#)[◀](#)[▶](#)[◀](#)[▶](#)[Back](#)[Close](#)[Full Screen / Esc](#)[Printer-friendly Version](#)[Interactive Discussion](#)

## Uncertainty contributions to low flow projections in Austria

J. Parajka et al.

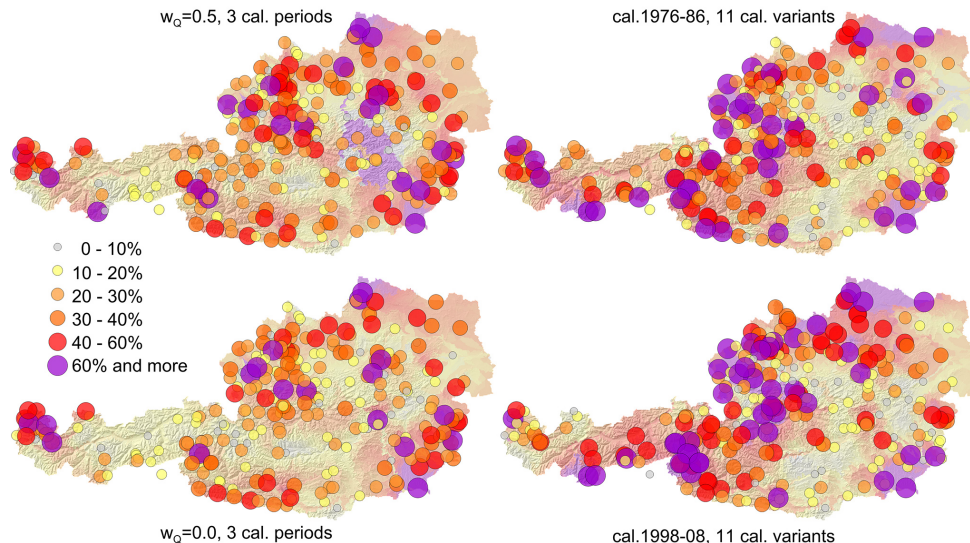


**Figure 6.** Uncertainty of  $Q_{95}$  model simulations estimated from 11 calibration variants calibrated in the same calibration period (right panels, top – calibration period 1976–1986, bottom – calibration period 1998–2008) and from three calibration periods calibrated by the same calibration variant (left panels, top  $w_Q = 0.5$ , bottom  $w_Q = 0.0$ ). The uncertainty is expressed as the range of relative differences (%) between simulated and observed  $Q_{95}$  obtained by particular calibration variants in the period 1976–2008. Colour patterns in the background show the interpolated ranges by using top-kriging method (Skoien et al., 2014).

Title Page

Abstract

Introduction

Conclusions

References

Tables

Figures

⏪

⏩

◀

▶

Back

Close

Full Screen / Esc

Printer-friendly Version

Interactive Discussion



## Uncertainty contributions to low flow projections in Austria

J. Parajka et al.

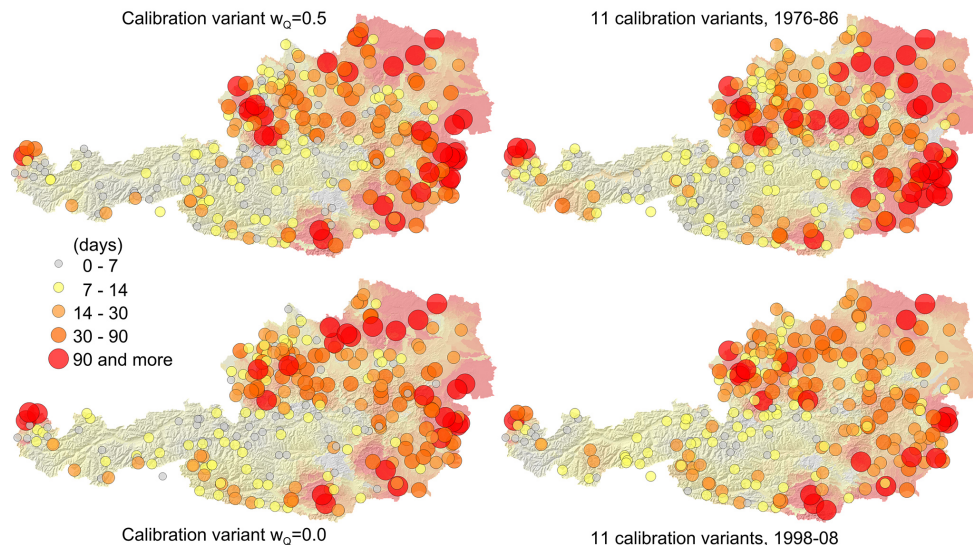


**Figure 7.** Uncertainty of simulations of low flow seasonality (SI) estimated from 11 calibration variants calibrated in the same calibration period (right panels, top – calibration period 1976–1986, bottom – calibration period 1998–2008) and from three calibration periods calibrated by the same calibration variant (left panels, top  $w_Q = 0.5$ , bottom  $w_Q = 0.0$ ). The uncertainty is expressed as the range of differences (days) between simulated and observed SI in the period 1976–2008. Colour patterns in the background show the interpolated ranges by using top-kriging.

Title Page

Abstract

Introduction

Conclusions

References

Tables

Figures

⏪

⏩

◀

▶

Back

Close

Full Screen / Esc

Printer-friendly Version

Interactive Discussion



## Uncertainty contributions to low flow projections in Austria

J. Parajka et al.

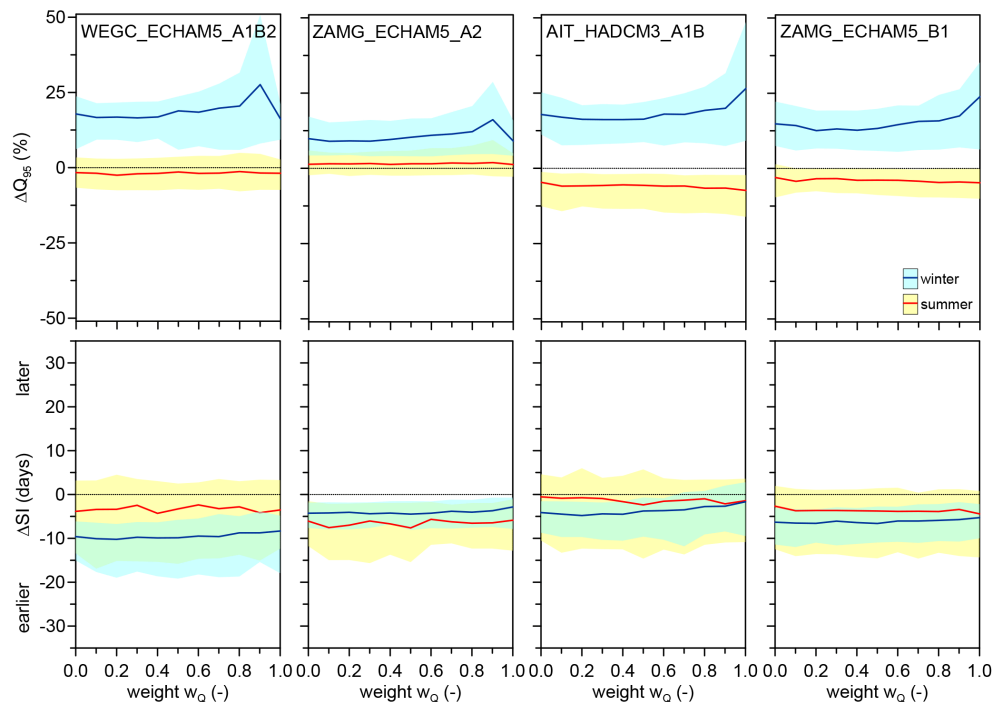


**Figure 8.** Projections of low flows for selected climate scenarios and calibration variants. Line represent the medians, scatter (i.e. 75–25% percentiles) show the variability over 262 basins. Top and bottom panels show projected changes of low flow quantiles  $Q_{95}$  and seasonality index SI in basins with winter (blue) and summer (orange) low flow regimes, respectively. Projections are estimated by a delta change approach and indicate changes in the period 2021–2050 with respect to the reference period 1976–2008. Calibration variants are calibrated in the period 1998–2008.

[Title Page](#)
[Abstract](#)
[Introduction](#)
[Conclusions](#)
[References](#)
[Tables](#)
[Figures](#)
[⏪](#)
[⏩](#)
[◀](#)
[▶](#)
[Back](#)
[Close](#)
[Full Screen / Esc](#)
[Printer-friendly Version](#)
[Interactive Discussion](#)


## Uncertainty contributions to low flow projections in Austria

J. Parajka et al.

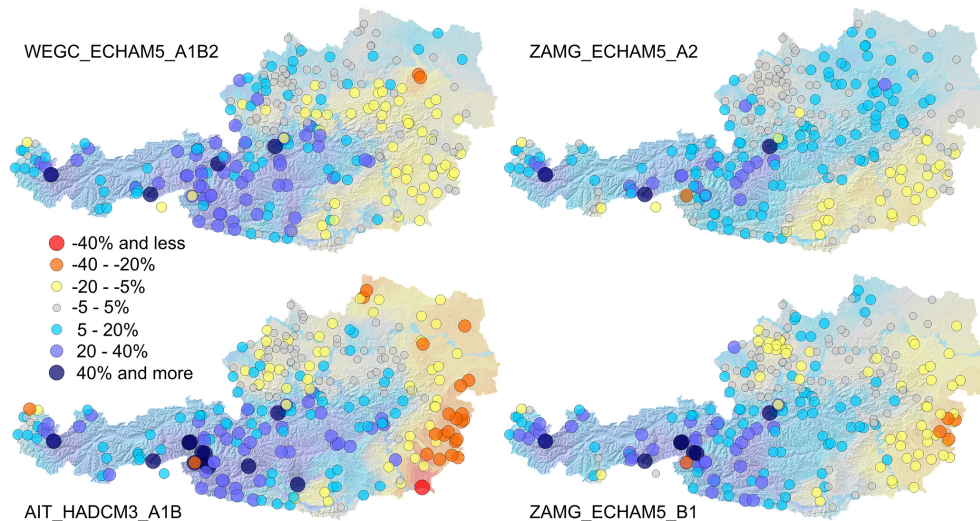


**Figure 9.** Projections of low flow quantiles  $Q_{95}$  changes for four climate scenarios in 262 Austrian basins. Projections show changes between future (2021–2050) and reference (1976–2008) periods. Model simulations are based on variant  $w_Q = 0.5$  calibrated in the period 1998–2008. Colour patterns in the background show the interpolated projections by using top-kriging.

[Title Page](#)
[Abstract](#)
[Introduction](#)
[Conclusions](#)
[References](#)
[Tables](#)
[Figures](#)
[⏪](#)
[⏩](#)
[◀](#)
[▶](#)
[Back](#)
[Close](#)
[Full Screen / Esc](#)
[Printer-friendly Version](#)
[Interactive Discussion](#)


## Uncertainty contributions to low flow projections in Austria

J. Parajka et al.

Title Page

Abstract

Introduction

Conclusions

References

Tables

Figures

◀

▶

◀

▶

Back

Close

Full Screen / Esc

Printer-friendly Version

Interactive Discussion

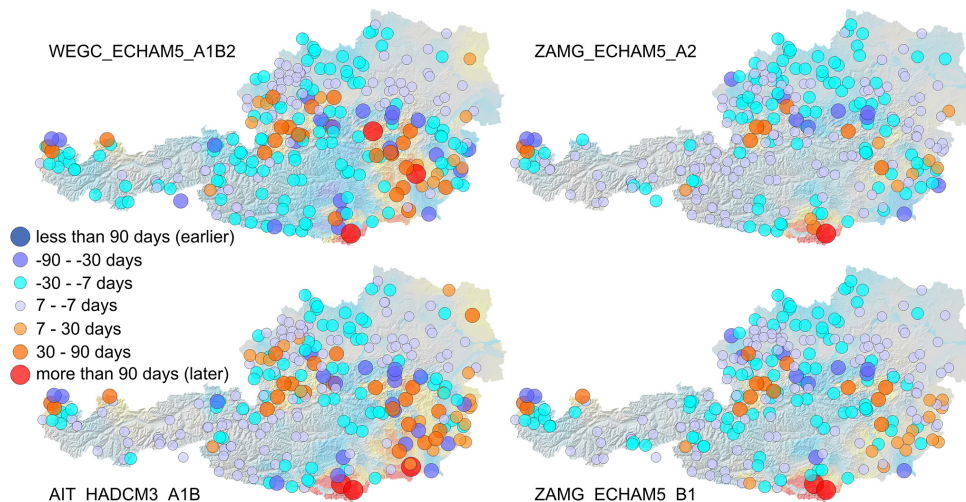


**Figure 10.** Projections of changes in low flow seasonality (SI) for four climate scenarios in 262 Austrian basins. Projections show changes between future (2021–2050) and reference (1976–2008) periods. Model simulations are based on variant  $w_Q = 0.5$  calibrated in the period 1998–2008. Colour patterns in the background show the interpolated projections by using top-kriging.

# HESSD

12, 12395–12431, 2015

## Uncertainty contributions to low flow projections in Austria

J. Parajka et al.

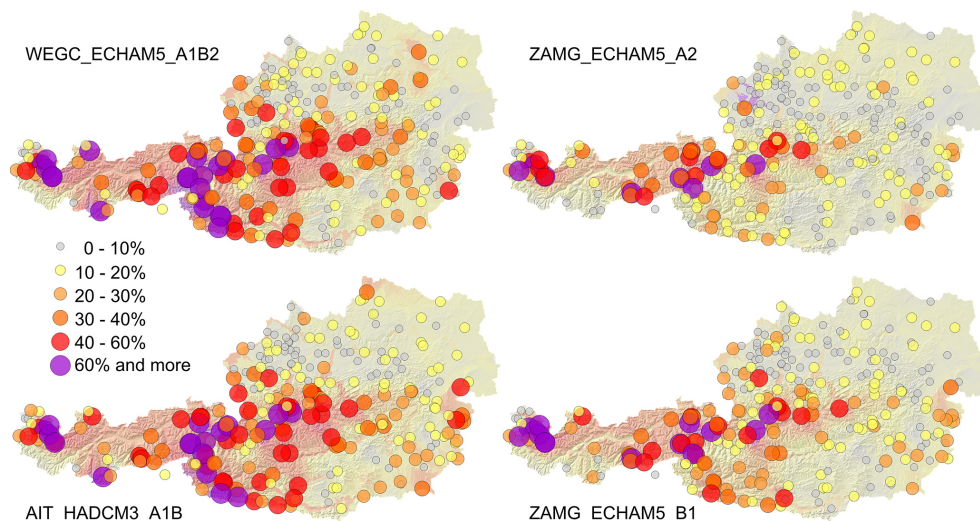


**Figure 11.** Uncertainty of  $Q_{95}$  model projections of low flows for four different climate scenarios. The uncertainty is expressed as the range of relative differences (%) between  $Q_{95}$  simulated in the future (2021–2050) and reference (1976–2008) period obtained for 11 calibration variants calibrated in three calibration periods. Colour patterns in the background show the interpolated ranges by using top-kriging.

Title Page

Abstract

Introduction

Conclusions

References

Tables

Figures

⏪

⏩

◀

▶

Back

Close

Full Screen / Esc

Printer-friendly Version

Interactive Discussion



## Uncertainty contributions to low flow projections in Austria

J. Parajka et al.

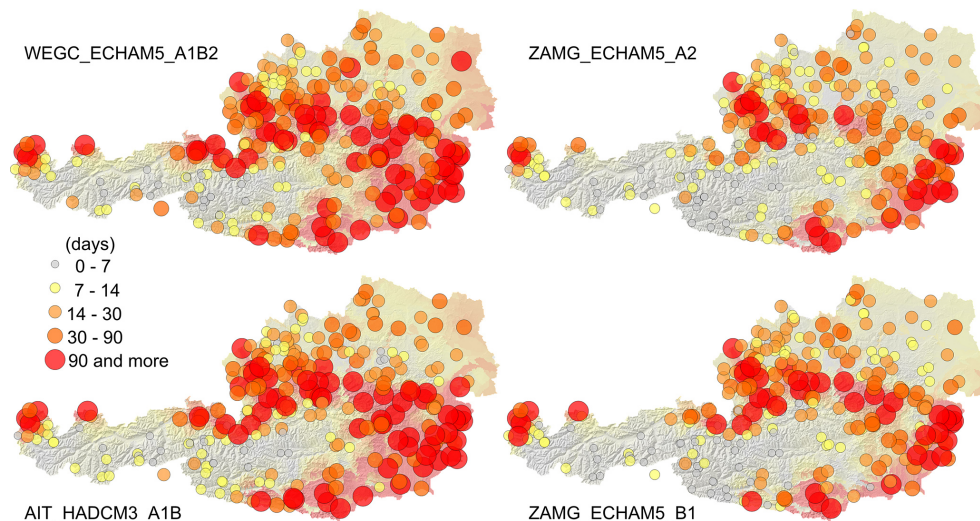


**Figure 12.** Uncertainty of model projections of low flow seasonality for four different climate scenarios. The uncertainty is expressed as the range of relative differences (%) between seasonality occurrence (SI) simulated in the future (2021–2050) and reference (1976–2008) period obtained for 11 calibration variants calibrated in three calibration periods. Colour patterns in the background show the interpolated ranges by using top-kriging.

Title Page

Abstract

Introduction

Conclusions

References

Tables

Figures

◀

▶

◀

▶

Back

Close

Full Screen / Esc

Printer-friendly Version

Interactive Discussion



## Uncertainty contributions to low flow projections in Austria

J. Parajka et al.

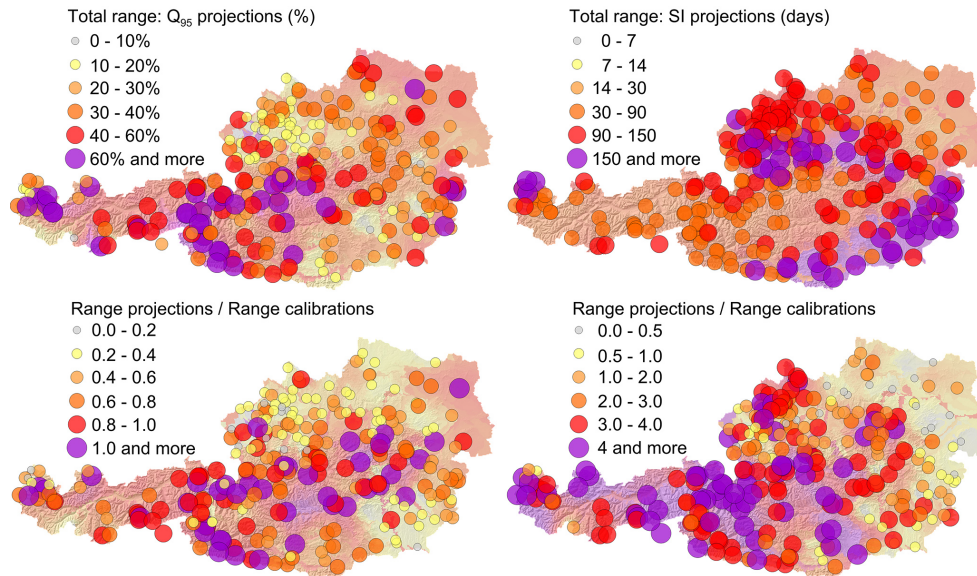


**Figure 13.** Total uncertainty of model projections of low flows for four different climate scenarios, 11 calibration variants and three calibration periods. The uncertainty is expressed as the range of  $Q_{95}$  (left panel) and seasonality (right panel) of differences between model simulations in the future (2021–2050) and reference (1976–2008) periods. Bottom panels show the ratio between the range of climate projections to the range of differences in the reference period. Colour patterns in the background show the interpolated ranges by using top-kriging.

[Title Page](#)
[Abstract](#)
[Introduction](#)
[Conclusions](#)
[References](#)
[Tables](#)
[Figures](#)
[◀](#)
[▶](#)
[◀](#)
[▶](#)
[Back](#)
[Close](#)
[Full Screen / Esc](#)
[Printer-friendly Version](#)
[Interactive Discussion](#)


## Uncertainty contributions to low flow projections in Austria

J. Parajka et al.

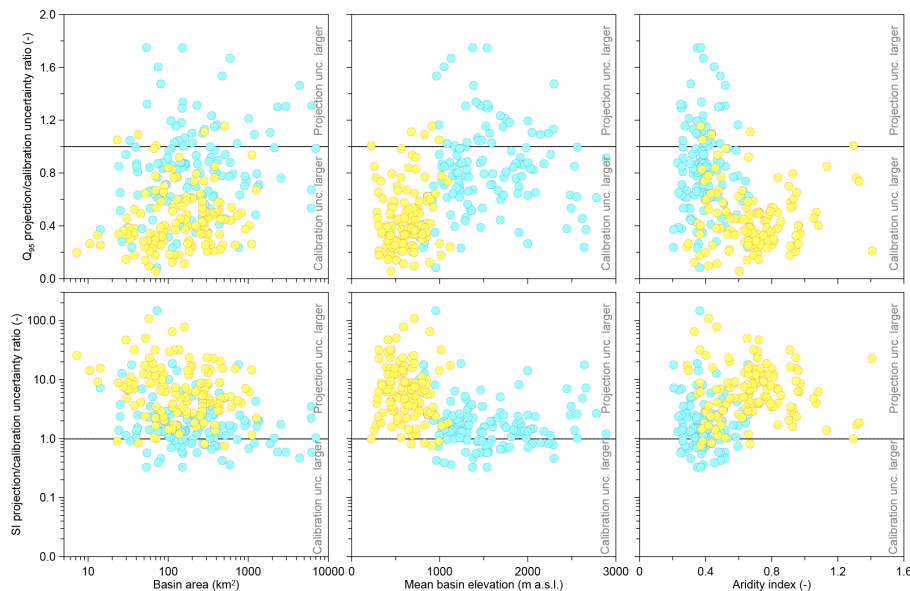


**Figure 14.** Relationship between the uncertainty ratio between calibration and projection uncertainty and basin area (left panels), mean basin elevation (middle panels) and aridity index (right panels). Top and bottom panels show the uncertainty ratio for the low flow quantile (Q95) and seasonality index (SI), respectively. Basins with winter low flow seasonality are plotted in blue, basins with summer low flow seasonality are in yellow.

[Title Page](#)[Abstract](#)[Introduction](#)[Conclusions](#)[References](#)[Tables](#)[Figures](#)[◀](#)[▶](#)[◀](#)[▶](#)[Back](#)[Close](#)[Full Screen / Esc](#)[Printer-friendly Version](#)[Interactive Discussion](#)